Electronic Supplementary Material (ESI) for Chemical Science.
This journal is © The Royal Society of Chemistry 2019

Supporting Information

Programming *in Situ* Accelerated DNA Walkers in Diffusion-Limited Microenvironments

Feng Chen, [†,‡] Jing Xue, [†,‡,§] Min Bai, [‡] Jing Qin, and Yongxi Zhao[*,‡]

[‡] The Key Laboratory of Biomedical Information Engineering of Ministry of Education, School of Life Science and Technology, Xi'an Jiaotong University, Xianning West Road, Xi'an, Shaanxi 710049, P. R. China

[§] State Key Laboratory for Mechanical Behavior of Materials, School of Materials Science and Engineering, Xi'an Jiaotong University, Xianning West Road, Xi'an, Shaanxi 710049, P. R. China

Table S1. Sequence information for oligonucleotides used in this study.

Name	Sequences (5′-3′) [a]
oG-DT	TAMRA-GACGCCAGTGTAoGCGAGATGCGTC$(T)_{15}$-SH
I-DT	FAM-GACGCCAGTGTIGCGAGATGCGTC$(T)_{15}$-SH
AP-R	Cy5-GACGCAACTGACTdUACGTGACGCGTC$(T)_{15}$-SH
DW	HS-$(T)_{42}$ATCTCGCTACACTG
Random DW	HS-$(T)_{42}$TAGCTTATCAGACT

[a] Red characters represent the DNA damage bases.

Supporting figures

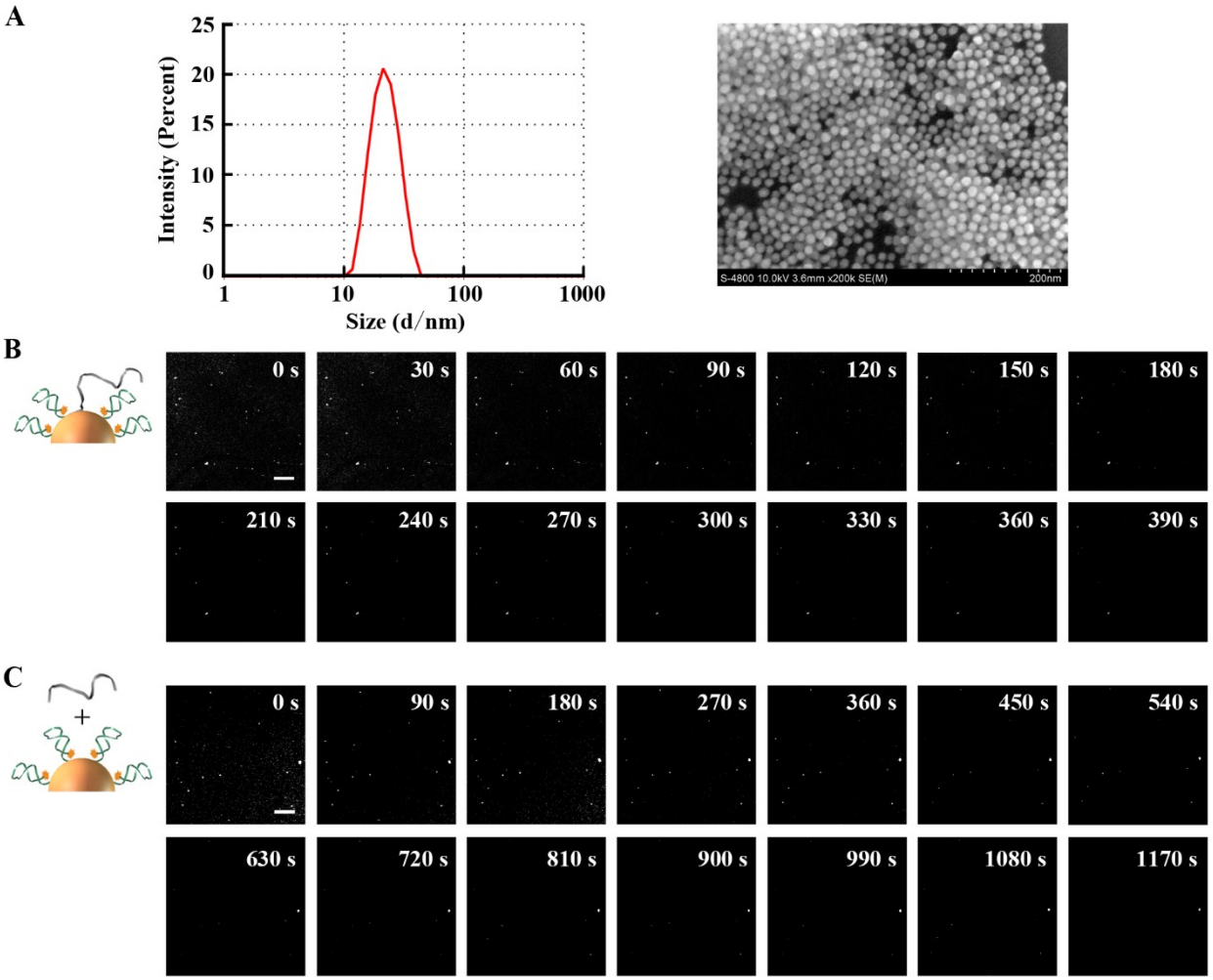

Figure S1. (A) Characterization of AuNPs before and after DNA functionalization. Left, DLS analysis of bare AuNPs; middle, SEM images of bare AuNPs. Time-lapse single-particle STED images for in situ accelerated DNA walkers (B) and (C) post-assembly control, scale bar = 5 μm. STED images of Figure 1A were selected from the big images above (0-360 s)

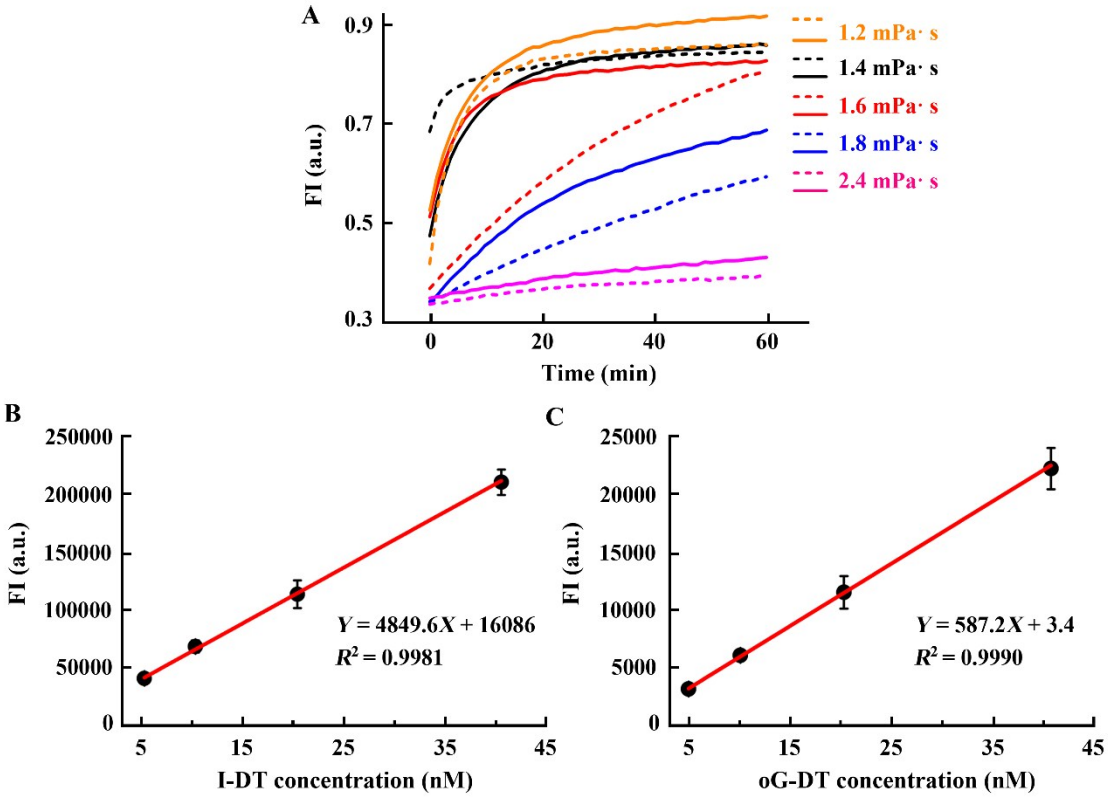

Figure S2. (A) Real-time fluorescence performance of *in situ* accelerated DNA walker (solid lines) and post-assembly control (dashed lines) in crowded solutions with different viscosity. (B, C) Standard curves for fluorescence intensity of I-DT and oG-DT with different concentrations, respectively. The standard curves were used to transform the fluorescence intensity to cleavaged DT concentration (or walking events). The initial walking velocity in Figure 1B was determined by the first 5 min of the real-time fluorescence curves.

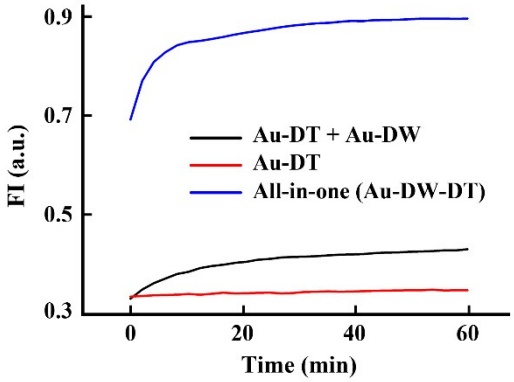

Figure S3. Verification of on-particle rather than interparticle DNA mobility of the proposed DNA walker. Au-DT, Au-DW and Au-DW-DT indicate AuNPs modified with DT, DW and DW/DT, respectively.

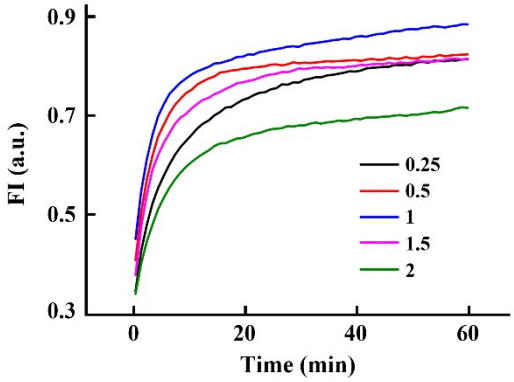

Figure S4. Real-time fluorescence intensity curves of single-track *in situ* accelerated DNA walker (controlled by hOGG1/APE1) with different on-particle DW densities. The unit of the density was DW number per 100 nm^2.

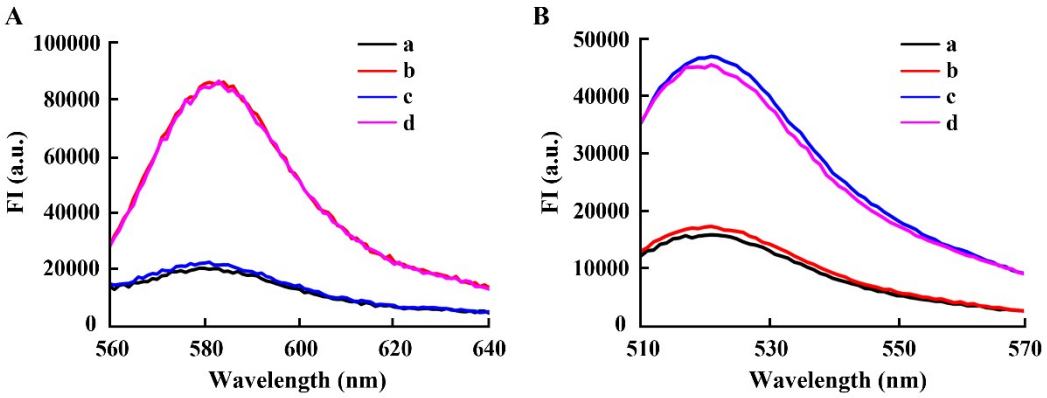

Figure S5. Fluorescence emission spectra of walking performance of the twin-track walker controlled by two pathways, (A) hOGG1/APE1 and (B) hAAG/APE1. Small letters represent (a) no hOGG1 or hAAG, (b) hOGG1 (4 U/mL), (c) hAAG (5000 U/mL) and (d) hOGG1 (4 U/mL) and hAAG (5000 U/mL).

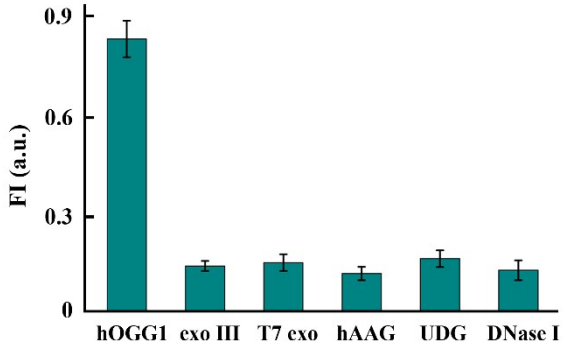

Figure S6. Selectivity of the *in situ* accelerated DNA walker powered by hOGG1/APE1. The reaction buffer contained 4 U/mL hOGG1, 50 U/mL exo III, 50 U/mL T7 exo, 50 U/mL hAAG, 50 U/mL UDG and 1 U/mL DNase I. APE1 (2000 U/mL) were used in this research. The error bars represent the standard deviations of three experiments.

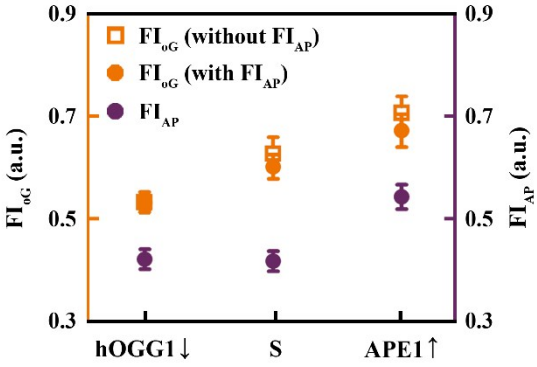

Figure S7. Analysis of the self-calibration function of AP-R probe for *in situ* accelerated DNA walker powered by hOGG1/APE1. Square box and solid circles each represent the fluorescence responses (F_{oG} and F_{AP}) of the walker modified without and with AP-R probe. Letter 'S' indicate the starting concentrations of enzymes (hOGG1 and APE1); Two arrows indicate the decrease of hOGG1 and increase of APE1, respectively. The error bars represent the standard deviations of three experiments.

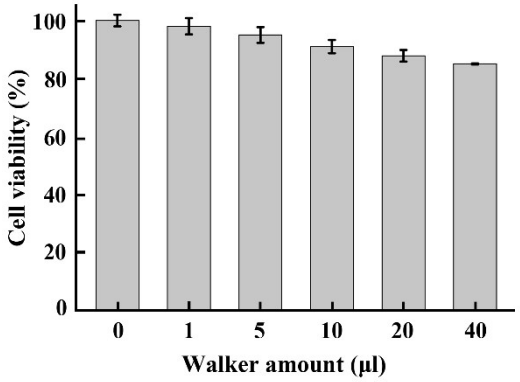

Figure S8. Cell viability assay for the investigation of cytotoxicity of proposed DNA walkers using 2,5-diphenyl tetrazolium bromide (MTT) test. 40000 HeLa cells per well were treated with DNA walker (twin-track) of different amount in DMEM (total volume of 200 μl, without FBS) at 37 °C for 12 h. The absorbance at 490 nm was measured by a microplate reader (Tecan Infinite F50).

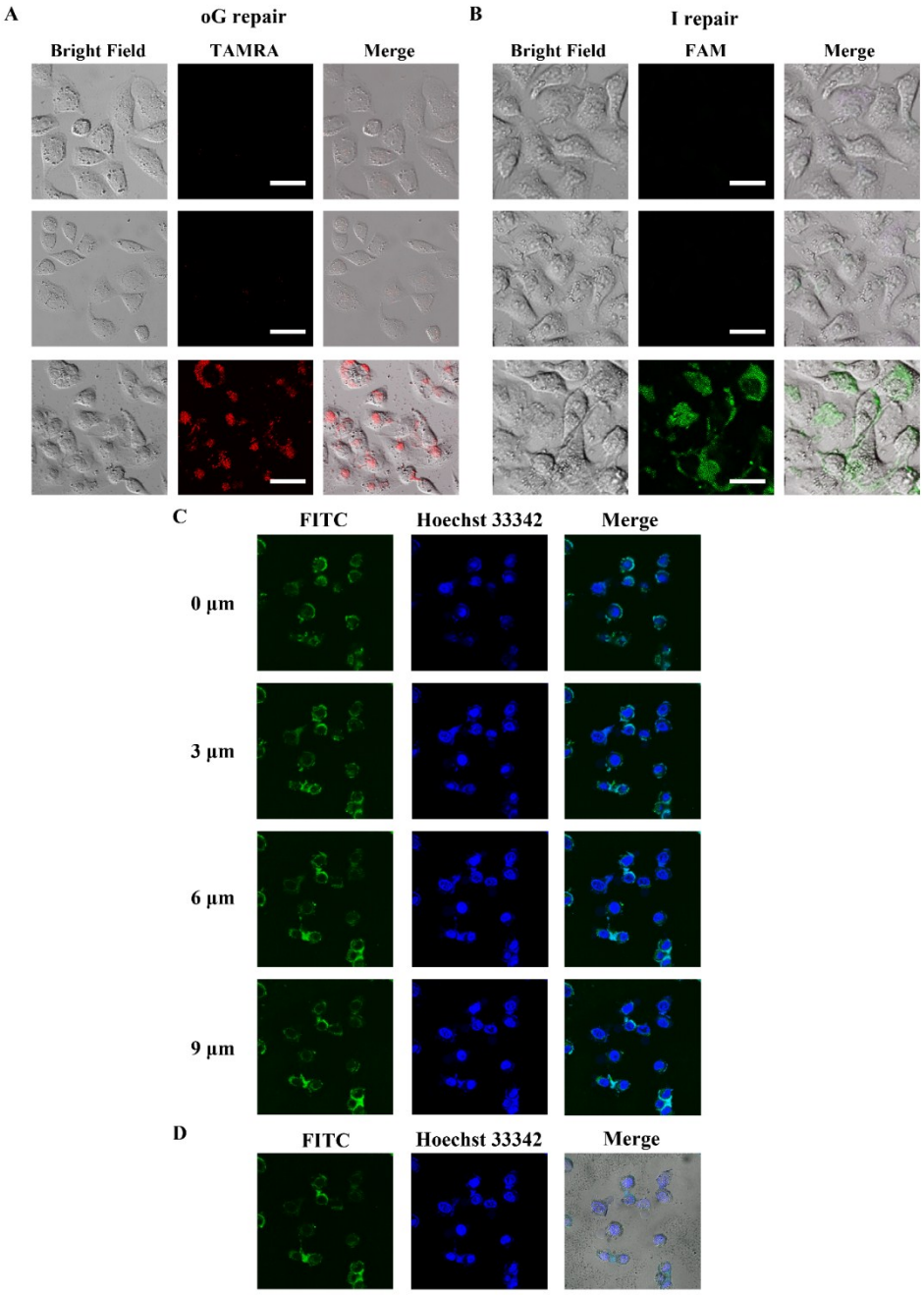

Figure S9. Intracellular fluorescence imaging of single-track *in situ* accelerated DNA walker. (A) and (B) are cell images monitoring guanine oxidation (G to oG) and adenosine deamination (A to I editing) damage repair, respectively. Top, DNA walker with DTs only; middle, DNA walker with random DW and DTs; bottom, DNA walker with specific DW and DTs. These images are corresponding to Figure 3. (C) Z-stack fluorescence images of Hoechst 33342-stained HeLa cells treated with DNA walker for monitoring adenosine deamination (A to I editing) damage repair. The nucleus (blue) were stained by Hoechst 33342 to confirm the internalization of DNA walkers into living cells. (D) The fluorescence images of the stack of 9 μm in (C) with merged bight field image.

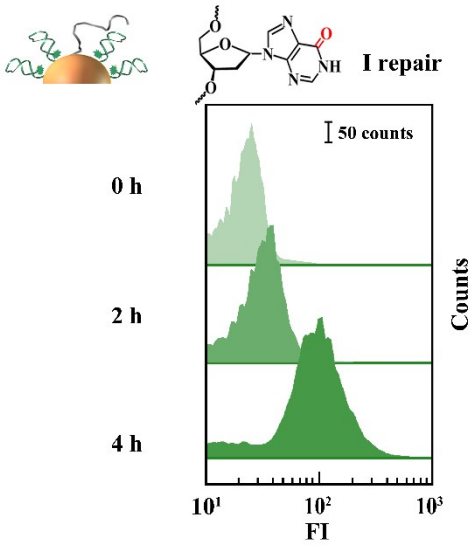

Figure S10. Flow cytometry data (scale bar of 50 counts in all three histograms) of HeLa cells incubated with *in situ* accelerated DNA walker for different time (0, 2 and 4 h, respectively). The reaction process was controlled by hAAG/APE1 pathway.

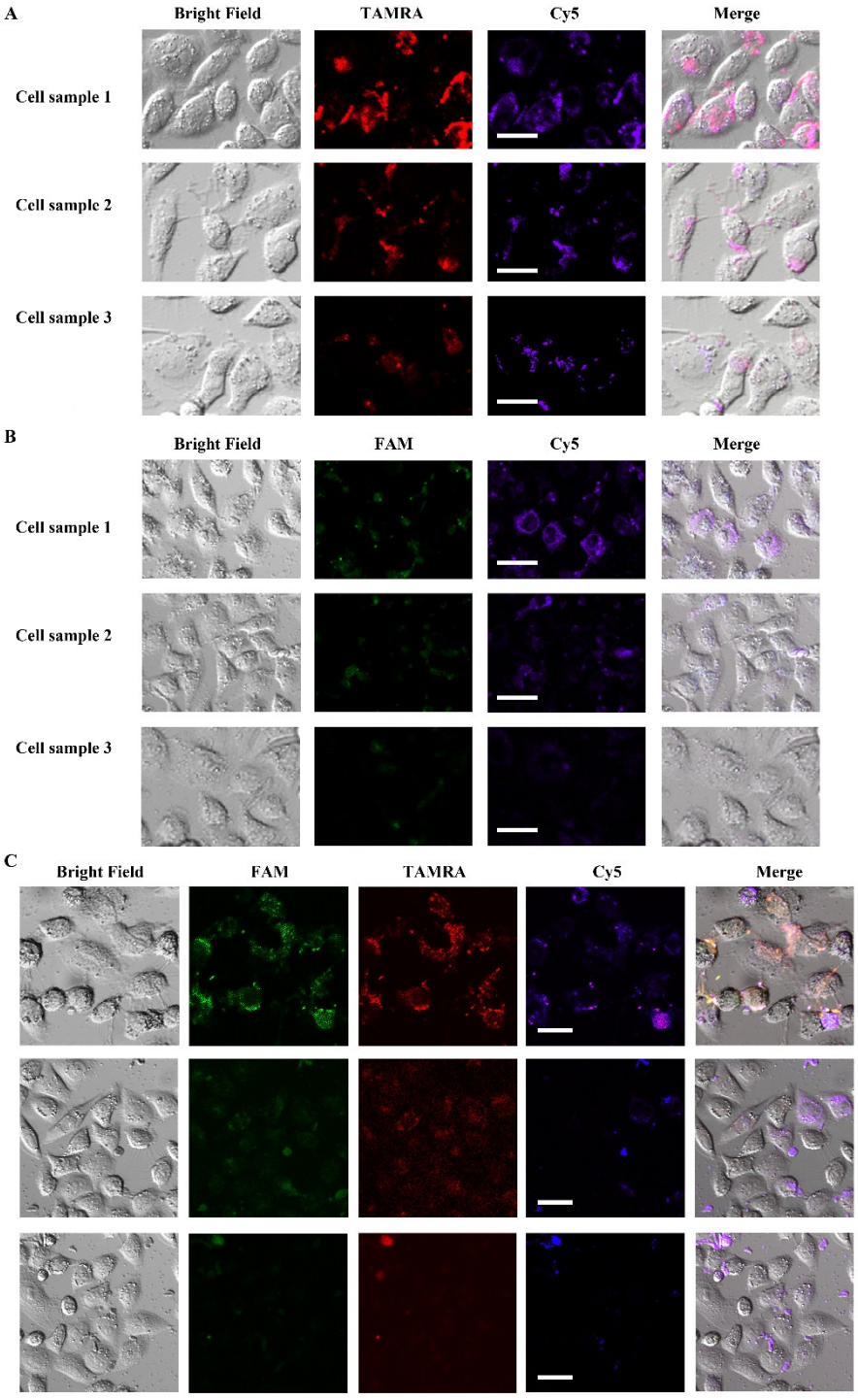

Figure S11. Self-calibration analysis of activities of intracellular glycosylases using *in situ* accelerated DNA walker. (A) Monitoring hOGG1 in cell samples with different APE1 activities (corresponding to Figure 4A). (B) Monitoring hAAG in cell samples with different APE1 activities. (C) Simultaneous monitoring of hOGG1 and hAAG in three cell samples with different APE1 activities using the twin-track walker (the top row corresponding to Figure 4B).